NISTIR 6449

A Water-to-Water Heat Pump Using Hydrocarbon and Hydrofluorocarbon Zeotropic Mixtures With and Without an Internal Heat Exchanger

W. Vance Payne, II
Eric A. Silk
Piotr A. Domanski

United States Department of Commerce
Technology Administration
National Institute of Standards and Technology
Building and Fire Research Laboratory
Gaithersburg, MD 20899

NISTIR 6449

A Water-to-Water Heat Pump Using Hydrocarbon and Hydrofluorocarbon Zeotropic Mixtures With and Without an Internal Heat Exchanger

W. Vance Payne, II
Eric A. Silk
Piotr A. Domanski

January 2000

Building and Fire Research Laboratory
National Institute of Standards and Technology
Gaithersburg, MD 20899

U.S. Department of Commerce
William M. Daley, *Secretary*
Technology Administration
Dr. Cheryl L. Shavers, *Under Secretary of Commerce for Technology*
National Institute of Standards and Technology
Raymond G. Kammer, *Director*

TABLE OF CONTENTS

List of Tables

List of Figures

Nomenclature

h	convective heat transfer coefficient
x	composition
Δ	change
UA	product of overall heat transfer coefficient and area

Subscripts

a	actual data
l	linearly interpolated
m	mixture
R1	refrigerant one
R2	refrigerant two
2ϕ	two-phase

A Water-to-Water Heat Pump Using Hydrocarbon and Hydrofluorocarbon Zeotropic Mixtures With and Without an Internal Heat Exchanger

W. Vance Payne II, Eric A. Silk*, and Piotr A. Domanski

Abstract

This investigation overviews the results of an experimental study pertaining to flammable refrigerant alternatives in water-to-water heat pumps for building and home applications. The system studied here used a secondary heat transfer loop to communicate with the indoor space. This isolates the flammable refrigerant in the outdoor section of the unit and demonstrates one configuration that could be accepted in the United States. In contrast to the fluid survey of the initial study (Payne *et al.*, 1999), the present study emphasizes the performance of R32/290, R22, R290, and R22-REF (direct expansion case) in the cooling and heating modes. The vapor compression cycle used an internal heat exchanger added between the liquid and vapor lines. Fluid performance as a function of thermophysical properties and heat transfer characteristics are addressed for each cycle configuration.

The heat pump charged with R32/290 had the closest performance to the R22 direct expansion system in the cooling mode. Furthermore, the internal heat exchanger system performance exceeded that of the basic vapor compression cycle configuration. In the heating mode, R290 in the basic configuration had the closest approximation to the R22 direct expansion performance. The application of the internal heat exchanger degraded R290's performance.

Keywords: Water-to-water heat pump, zeotropic mixtures, flammable refrigerants, COP

---

* Research Assistant from University of Maryland, Center for Environmental Energy Engineering, College Park, Maryland

1: Introduction

Didion (Mulroy *et al.*, 1988) originally proposed the use of zeotropic mixtures in the water-to-water heat pump as a method for improving heat pump performance for low-lift/high-glide applications. A later simulation study showed that the coefficient of performance, COP, of the water-to-water system charged with a zeotropic mixture can approach the COP of the direct-expansion R22 system if large counter-flow heat exchangers are used as the evaporator and condenser (Domanski *et al.*, 1994). The follow-up experiment in a general-purpose mini-breadboard heat pump (MBHP) showed the importance of adequate sizing of the heat exchangers (Choi *et al.*, 1996). The evaporator and condenser of the MBHP did not have sufficient capacity to obtain a sizable gain in COP due to glide matching between the zeotropic mixture and heat-transfer fluid.

In this study an internal heat exchanger (ICHX) was used to exchange heat between the high-pressure refrigerant leaving the condenser and two-phase refrigerant leaving the evaporator. The name ICHX is used instead of "liquid line/suction line heat exchanger " to emphasize that a two-phase flow refrigerant participates in the heat transfer although the designs of both heat exchangers are basically the same. The current study was also performed in a specially designed apparatus with a large brazed plate evaporator and condenser to ensure adequate capacity.

The use of an ICHX with zeotropic mixtures was originally outlined by Vakil (1981). The benefit of using the ICHX with zeotropes stems from the fact that zeotropic mixtures have a temperature glide while evaporating or condensing at constant pressure. Increased condenser subcooling results in a lower enthalpy at the entrance of the evaporator. For a fixed system capacity, the average fluid-to-refrigerant temperature difference will be a constant, the evaporation process will start at a lower quality, and the evaporator pressure will increase. This increase in pressure reduces the pressure ratio seen by the compressor, thus lowering the compression work. However, an increase in the COP is only observed for fluids with high molar heat capacity (Domanski, 1995).

Isolation of the flammable refrigerant in the outdoor section of the heat pump allows these refrigerants to be included in the list of alternatives for R22. The application of zeotropic mixture glide matching, larger heat exchangers, and internal refrigerant cycle heat transfer seeks to remove the added temperature lift penalty associated with an indoor secondary heat transfer fluid loop. The current study uses both large heat exchangers and the concept of internal heat exchange to maximize the performance of zeotropic blends. Using the internal heat exchanger in the refrigerant cycle in addition to glide matching between the secondary heat transfer fluids and the refrigerant produced increases in COP. The configuration under study does not exclude flammable refrigerants because the refrigerant charge is isolated outdoors along with all of the vapor compression cycle components.

2: Experimental Setup

The experimental setup consisted of four main subsystems; the vapor-compression system, the indoor heat transfer fluid loop, the outdoor heat transfer fluid loop, and the ground loop. A detailed description of all sub-loops is provided by Payne et al. (1999). For clarity of presentation, a description of the vapor-compression system with the ICHX is also included in this report.

2.1: Vapor-compression System

Figure 2.1 shows a schematic of the vapor-compression system with the intracycle heat exchanger. The system consisted of a reciprocating compressor, condenser, a manually adjustable expansion device, evaporator, and an accumulator. The compressor was a two-cylinder open-drive reciprocating design displacing from 3.53 m^3/h (2.08 cfm) to 21.76 m^3/h (12.81 cfm) with minimum speed of 500 rpm and maximum speed of 3 000 rpm. Compressor bore was 55 mm (2.16 in) and stroke was 49 mm (1.93 in). The intracycle heat

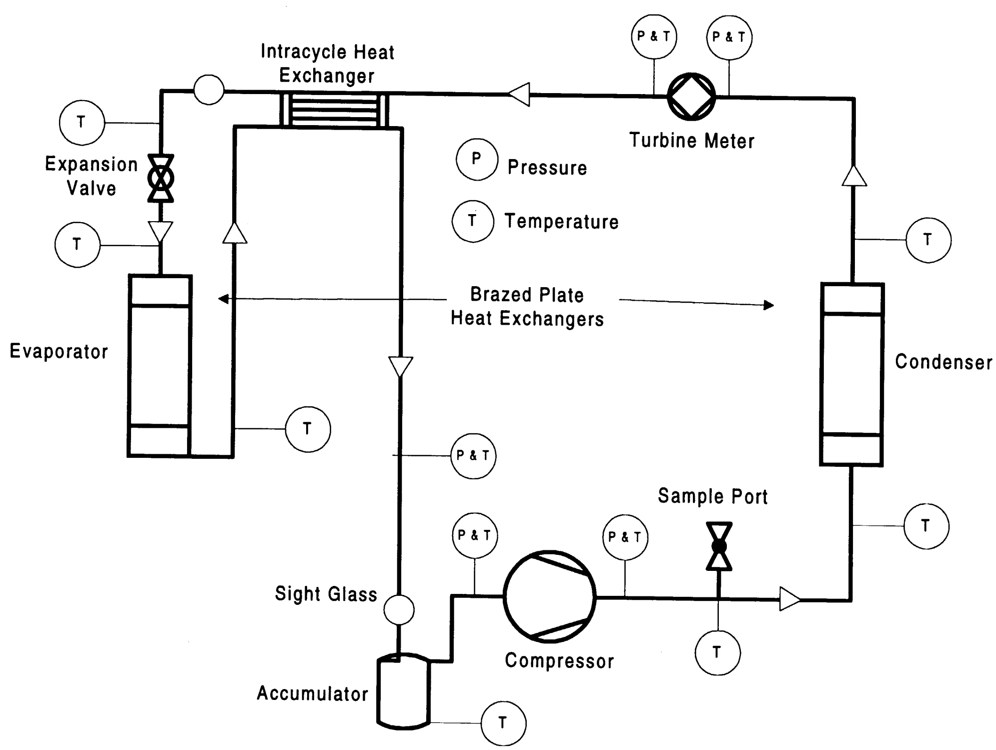

Figure 2.1: Vapor-compression system with intracycle heat exchanger

exchanger consisted of two conventional liquid line-to-suction line heat exchangers in series. One of the intracycle heat exchangers could be bypassed, and each heat exchanger was sized for a 10.6 kW (36 000 Btu/h) R22 cooling system. The brazed plate heat exchangers were installed to provide for counter-flow heat exchange between the refrigerant and a 70/30 by mass water/ethylene glycol heat transfer fluid. The system was designed for a cooling load of 10.6 kW (36 000 Btu/h). The high pressure refrigerant tubing was copper with 12.7 mm OD

(0.5 in) and 9.5 mm ID (0.375 in). The low pressure refrigerant tubing was copper with 15.9 mm OD (0.625 in) and 12.7 mm ID (0.5 in). The compressor was driven by an 11.2 kW (15 hp) explosion-proof motor coupled to the compressor shaft through a torque and RPM transducer. The motor speed was controlled by a variable frequency drive. The motor was oversized to compensate for the loss of torque at high frequency. The use of an open drive compressor removed the motor power consumption from COP calculations and did not affect vapor superheat entering the compression cylinders.

2.2: Experimental Uncertainty

All tests were conducted under steady-state conditions. For cooling tests, steady state occurred after one hour and when a steady stream of condensate was being produced by the indoor heat exchanger. For the heating tests, the heat pump was operated for one hour after indoor room conditions were stable. The expanded uncertainty for all measurements was estimated using the propagation of uncertainty through the appropriate equations. All expanded uncertainties are reported for a 95 % confidence interval and are evaluated by statistical methods. The estimates shown below were calculated for typical test conditions and are median values of the expanded uncertainty. A detailed development of the expanded uncertainty for this study may be found in Payne *et al.,* (1999).

Table 2.1: Measurement uncertainty for typical tests

Performance Parameter	Value	95 % Confidence Limit on Mean
COP	5.3	2.7 %
Capacity	9.10 kW (31036 Btu/h)	2.4 %
COP	5.0	3.9 %
Capacity	6.78 kW (23120 Btu/h)	3.7 %
COP	4.4	14.1 %
Capacity	2.71 kW (9261 Btu/h)	14.0 %
COP	6.5	15.3 %
Capacity	3.11 kW (10619 Btu/h)	15.2 %

3: Experimental Procedure

3.1: Test Procedure

The internal heat exchanger, ICHX, tests were carried out under the same conditions as specified for the basic cycle tests (Table 3.1). The only difference was the state of the refrigerant exiting the evaporator. For all of the ICHX tests, the refrigerant was not superheated; it left the evaporator at 90 % ± 5 % quality. This two-phase refrigerant then entered the ICHX, subcooling the liquid refrigerant exiting the condenser at a subcooling of 3.9 K (7.0 °F). The extent of the additional subcooling depended upon the mass flowrate of the refrigerant and whether both intracycle heat exchangers were in operation. The intracycle heat exchangers were selected to give a 3.9 K (7.0 °F) superheat at the entrance to the accumulator.

Table 3.1: Cooling conditions for all tests

Location	Setpoint	Tolerance
Indoor Dry-bulb Temperature	26.7 ° C (80 ° F)	±0.3 K (±0.5 ° F)
Indoor Dewpoint Temperature	15.8 ° C (60.4 ° F)	±0.3 K (±0.5 ° F)
Condenser HTF Inlet Temperature	25.0 ° C (77.0 ° F)	±0.3 K (±0.5 ° F)
HTF Temperature Differences Across the Evaporator and Condenser	5.6 K (10.0 ° F)	±0.3 K (±0.5 ° F)
Refrigerant Evaporator Superheat and Condenser Subcooling	3.9 K (7.0 ° F)	±1.1 K (±2.0 ° F)

ICHX heating tests were performed just as they were for the basic refrigeration cycle. The heat transfer fluid, HTF, flowrates were reversed with cooling test condenser flowrate being met in the evaporator and cooling test evaporator flowrate being met in the condenser. The same number of ICHXs used in the cooling tests were used for the heating tests. Refer to Payne *et al.* (1999) for a complete description of the basic configuration test procedures and conditions.

Table 3.2: Heating test conditions

Location	Setpoint	Tolerance
Indoor Dry-bulb Temperature	21.1 ° C (70.0 ° F)	±0.3 K (±0.5 ° F)
Indoor Dewpoint Temperature	12.06 ° C (53.7 ° F) maximum	±0.3 K (±0.5 ° F)
Evaporator HTF Inlet Temperature	0.0 ° C (32.0 ° F)	±0.3 K (±0.5 ° F)
HTF Temperature Differences for the Evaporator and Condenser	NA	NA
Refrigerant Evaporator Superheat and Condenser Subcooling	3.9 K (7.0 ° F)	±1.7 K (±3.0 ° F)

The ICHX was implemented in the refrigerant loop for both modes. Its application was used in two different manners.

3.2: Refrigerants Tested

The fluids surveyed in the ICHX system configuration were R32/290, R290, and R22. R32/290 and R290 were the best performers in the initial study for the cooling and heating modes respectively. R22 was investigated because it was used as the baseline fluid (direct expansion model fluid) in the initial study. Table 3.3 presents selected properties of the tested refrigerants with refrigerant properties calculated using REFPROP (NIST 1996).

Table 3.3: Selected properties of tested refrigerants at 4.4 °C (40 °F) saturation temperature[a]

Name	GWP[b]	ASHRAE Standard 34 Safety Group	Vapor Pressure [c] kPa (psia)	$T_{dew} - T_{bub}$ K, (° F) [c]	Liquid Thermal Conductivity W/(m K) (Btu/(h ft °F))	Vapor Absolute Viscosity kg/(m s) (lb/(ft h))	Volumetric Capacity kJ/m^3 (Btu/(ft^3))
R22	1500	A1	574.3 (83.3)	0	0.09467 (0.0547)	11.891x10^{-6} (.02873)	4895.8 (131.4)
R290	20	A3	541.9 (78.6)	0	0.10395 (0.06006)	7.81836x10^{-6} (0.01889)	4344.4 (116.6)
R32/290 (50/50)	335	A2 / A3	976.9 (141.69)	5.7 (10.3)	0.12015 (0.06942)	9.70569x10^{-6} (.02345)	8532.3 (229.0)
R32/152a (50/50)	395	A2 / A2	551.6 (80.0)	7.9 (14.2)	0.13062 (0.07547)	1.05707x10^{-6} (.02554)	5059.8 (135.8)
R290/600a (70/30)	20	A3 / A3	415.4 (60.25)	6.6 (11.9)	0.10516 (0.06076)	7.599x10^{-6} (0.01836)	3524.7 (94.6)

[a] From REFPROP 5.16 (NIST 1996)

[b] integrated time horizon 100 years; CO_2 as reference

[c] zeotropic mixture pressure at a 4.4 °C (40 °F) average of dew and bubble temperatures

4: Experimental Results

4.1: Basic Test Summaries

While the primary emphasis of this study was the performance impact due to internal heat exchange, much insight was gained from the results of the basic cycle study that did not include the intracycle heat exchanger (Payne *et al.*, 1999). These insights were based on the fluid rankings, and the thermophysical and transport properties of the fluids surveyed. The fluid performance in the basic cycle study provided a gauge for determining the impact of intracycle applications. With this in mind, the results from the basic tests have some bearing upon the conclusions of the intracycle tests. In the basic cycle study, the fluids surveyed could be categorized into three different analysis groups. Those groups were pure fluids vs. pure fluids, pure fluids vs. mixtures, and mixtures vs. mixtures.

Figure 4.1 displays a summary plot for the basic configuration cooling mode tests. None of the fluids produced a higher COP than the experimentally simulated direct expansion indoor coil case of R22-REF. With regard to the pure fluids, R290 performed better than R22 throughout the cooling capacity regime. R22 had a much higher density than R290; thus it required fewer compressor revolutions to achieve the same capacity as R290. While evaporator pressures where approximately the same at corresponding capacities, condenser pressures for R290 were lower then those for R22. Examination of the UA values also revealed that those for R290 were consistently higher than those for R22.

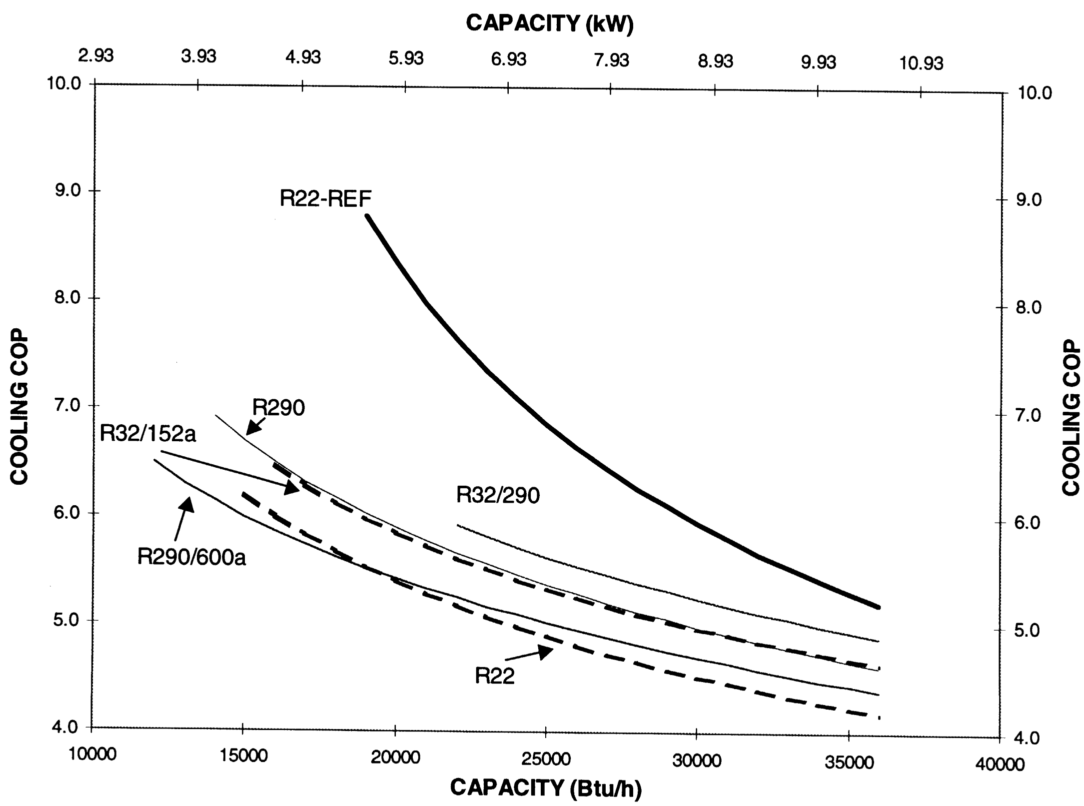

Figure 4.1: Cooling COP as a function of capacity; basic cycle

Comparison of the mixture COPs in Figure 4.1 shows that R32/290 and R32/152a both performed better than R290/600a. General COP rankings for the mixtures correspond directly with the volumetric capacities of the fluids (highest to lowest). For rankings see Payne *et al.*, 1999. R290/600a had the lowest COP of the three mixtures. R32/290 performed the best, while R32/152a ranked second. R32/290 had the highest COP of all the fluids surveyed and had the highest volumetric capacity as well. All of the fluids performed better than R22 throughout the capacity range shown.

Figure 4.2 displays heating COP as a function of capacity for the basic cycle that did not include the internal heat exchanger. The mixture COPs were much the same as in the cooling mode results. R32/290 and R32/152a both had higher COPs than R290/600a. Furthermore, R32/290 performed better than R32/152a throughout the capacity range above 5.3 kW (18 000 Btu/h). Below this value, R32/152a had a higher COP than R32/290. R290 also performed better than R22 in this case. The thermophysical trends and heat transfer characteristics witnessed in the cooling mode are also present here. R290 and R22 performed better than the other fluids with producing higher COPs than R22-REF in the 7.0 kW (24000 Btu/hr) capacity range. The R290 trace shows a performance within 5 % of that of the reference curve at higher capacities.

One possible explanation for the performance difference between R290 and R290/600a was advanced by Kedzierski et al. (1992). Their investigation showed that the convection coefficient for a mixture can be approximated as a linear interpolation between the values of the individual constituents.

$$h_{2\phi,linear} = x_m h_{R2} + (1 - x_m) h_{R1}$$

It has been found that degradation of the convection coefficient in the two-phase region may occur (Kedzierski et al., 1992). With this degradation, the convection coefficient is better represented as:

$$h_{2\phi,actual} = x_m h_{R2} + (1 - x_m) h_{R1} + \Delta h_{2\phi}$$

The degradation is imposed by a negative $\Delta h_{2\phi}$ term. The $\Delta h_{2\phi}$ value is a function of the constituent fluids and their compositions. Concentration gradients in the fluid are the primary cause of the degradation. The driving potential for concentration gradients is the difference between the liquid and vapor compositions in the fluid. The more volatile constituent of a binary mixture is considered to be the dominant component in determining the heat transfer degradation of a mixture. The molecular size of the more volatile constituent controls the diffusion rate of the concentration gradients. Smaller molecules imply larger diffusion rates and lower degradations (Kedzierski *et al.*, 1992). In the case of R32/290, R32 is the more volatile constituent; its small molecular size leads to a small heat transfer coefficient degradation, and it would tend to dominate in the mixture. For the basic cycle tests, R290 was used as a mixture constituent twice. The mixtures were R32/290 and R290/600a. Figure 4.1 shows that there was a COP degradation for R290/600a, and a COP improvement in the case of R32/290. The lowering of the R290 COP when R600a is added and the increasing of the COP when R32 is added could be caused by the mechanisms hypothesized by Kedzierski et al. (1992).

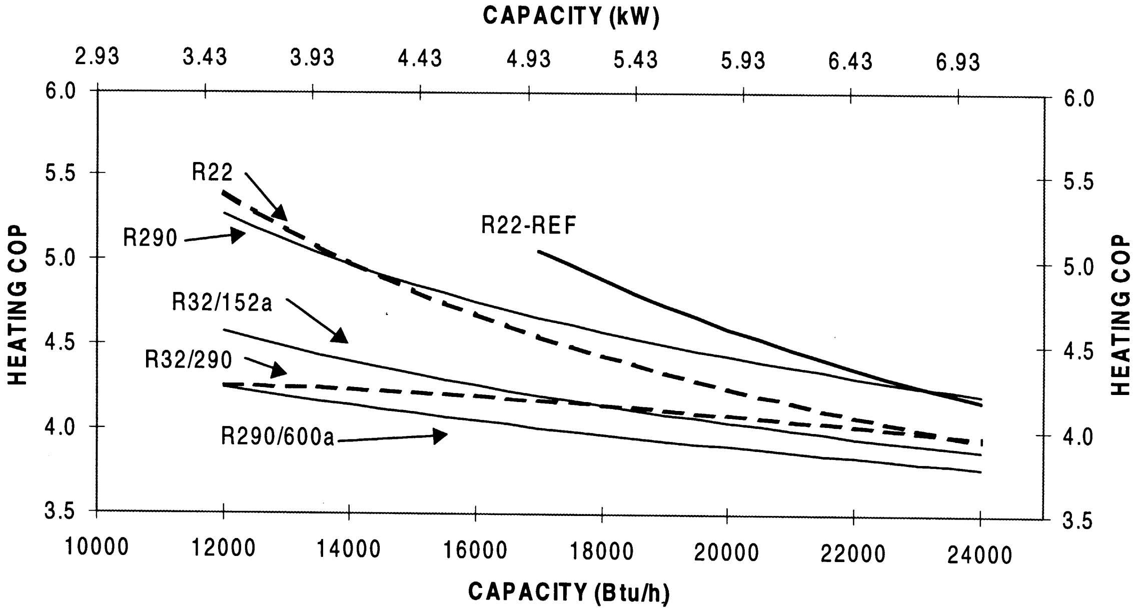

Figure 4.2: Heating COP as a function of capacity; basic cycle

4.2: Intracycle Study: suction line HX superheated/ internal HX configuration

The highest COPs for the basic configuration's (no internal heat exchanger) heating and cooling cases (R290 and R32/290 as well as R22) were further tested in the intracycle configuration, ICHX. Of primary interest was the ability of these fluids to approximate the R22-REF case COP or possibly exceed it. The fluids were tested in two different manners with the internal heat exchanger. The first had superheated vapor at the evaporator exit. The second had two-phase fluid exiting the evaporator. By having two-phase fluid exit the evaporator, the evaporator pressure will increase, and there will be an increase in the efficiency of the system (Domanski and Kim, 1996).

Figure 4.3 is a summary of the R32/290 cooling mode tests for all of the configurations studied. Curve fits were placed through the data points for ease of distinguishing the data trends. The middle line is for the basic configuration. Application of the ICHX with superheat caused a nominal decrease in COP of 4 % compared to the basic cycle with no internal heat exchanger. This is displayed by the bottom line. This was the lowest COP case. The ICHX application (two-phase at the evaporator exit) was the best case scenario, and it improved upon the COP of the basic and superheated configuration by 2 % and 6 %, respectively. The top line represents the ICHX data. There was a pressure drop on the vapor side of the heat exchanger when implementing the superheated mode. However, this pressure drop was negated when using the ICHX in the two-phase mode. Maximum COP's were achieved at the lower capacities for each case.

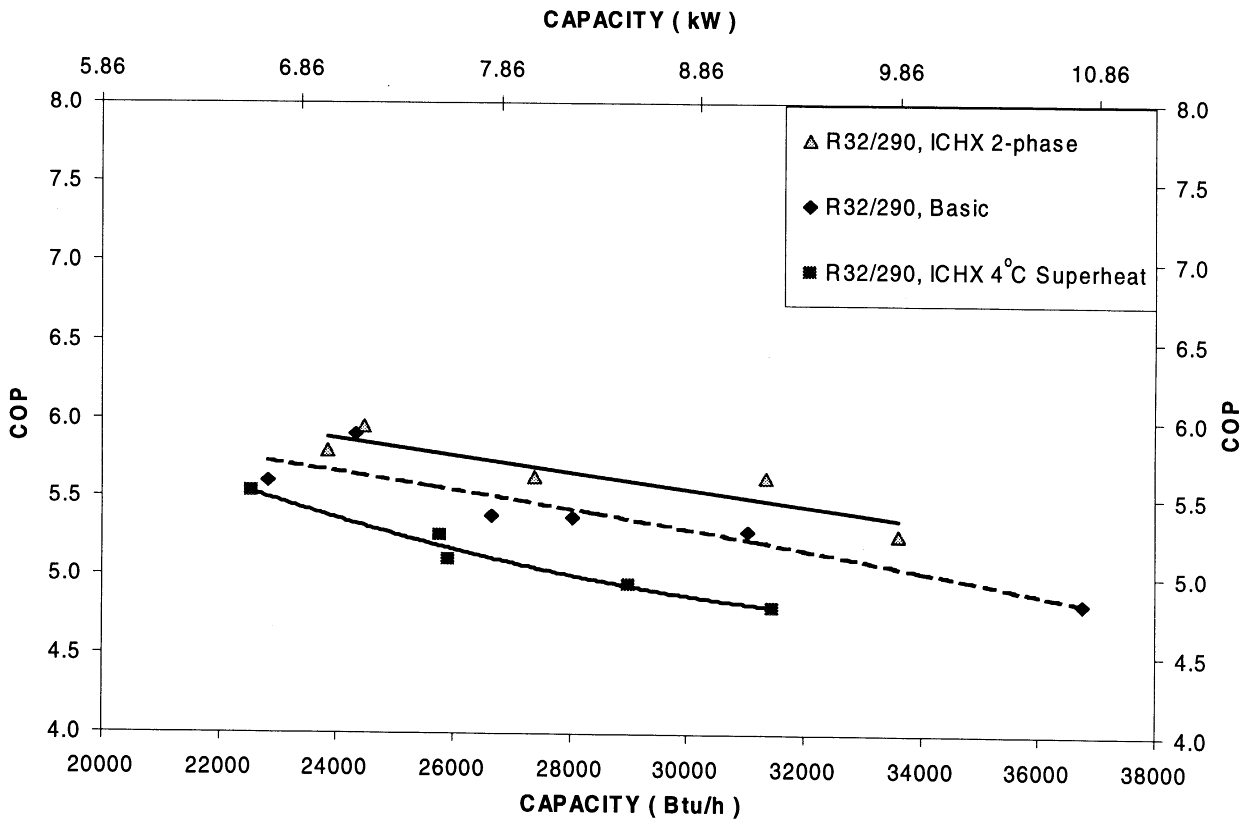

Figure 4.3: Cooling COP as a function of capacity for R32/290 basic and intracycle configuration

During the heating mode tests with no internal heat exchanger, R290 had the highest COP. Thus R290 was the primary fluid of interest in the intracycle heating mode study. Figure 4.4 displays a summary plot for the COP of R290 in the various cycle configurations. R290 experienced a different impact from the application of the internal heat exchanger than did R32/290. Here, the COP degraded with the application. This occurred in the cooling mode as well. The best performance (top curve) was for the basic configuration. Performances for the intracycle heat exchanger applications were nearly identical. This is displayed in the plot by the two bottom overlay lines. The basic configuration performed 5 % better than when the internal heat exchanger was used. Lower COP was partly due to pressure drop through the intracycle heat exchanger.

Figure 4.5 displays cooling mode COP's for all of the refrigerants tested with the internal heat exchanger. The original R22-REF test is included as well for purposes of comparison. The lowest COP was produced by R22. The R32/290 ICHX (two-phase leaving evaporator) configuration had a higher COP than R22, ranging from 16 % to 22 % higher over a comparable capacity range. However, even with the enhanced cycle and substantial improvement, R32/290 ICHX was still not able to fully compensate for the penalty of the additional indirect heat exchange loop. The R32/290 COP deficit varied from 19 % to 4 % lower than R22-REF.

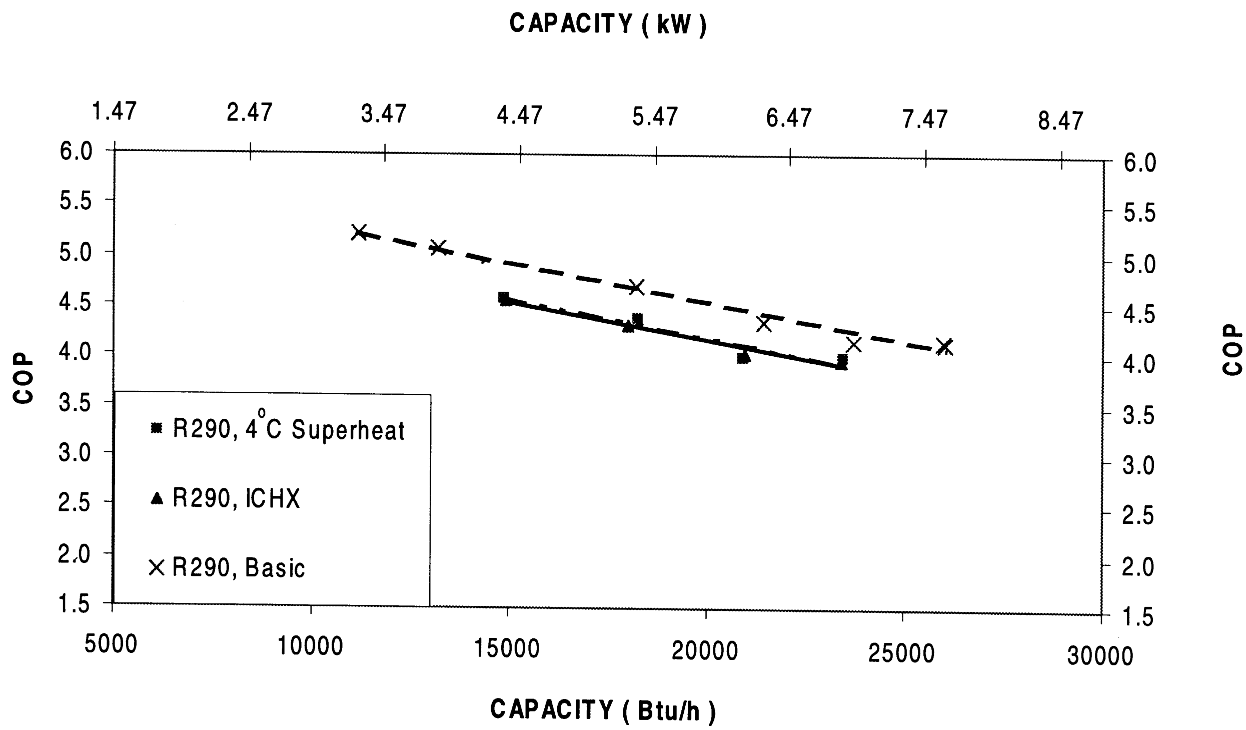

Figure 4.4: R290 heating mode COP's for basic and intracycle configuration

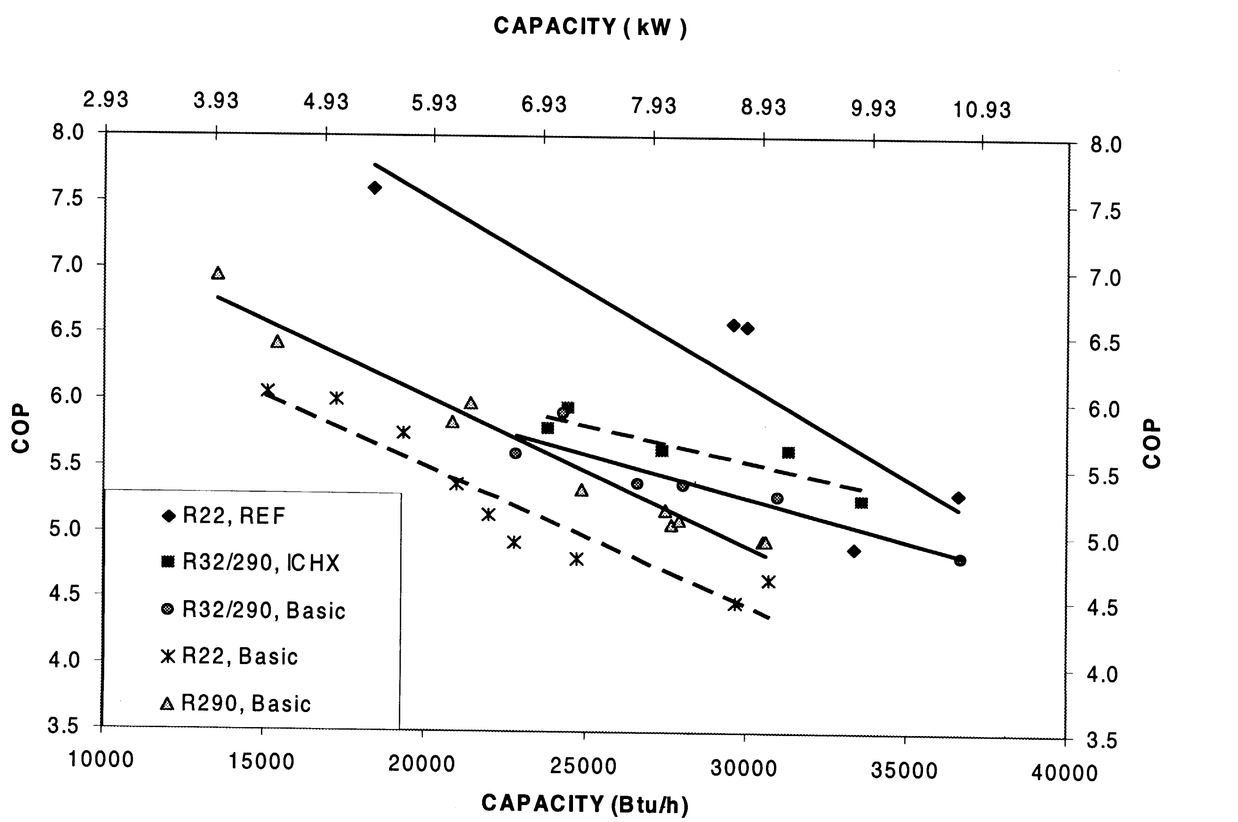

Figure 4.5: Comparison of cooling COP's for R22, R290, and R32/290

Figure 4.6 displays a summary plot for the refrigerants tested in the enhanced cycle heating mode study. Linear fits have been drawn through the selected data points. Given that the internal heat exchanger superheated and intracycle applications degraded performance, the best case (basic) configurations have been plotted here for R22 and R290. While R32/290 basic had the lowest COP of the fluids surveyed, it did experience an improvement of greater than 8 % in the ICHX (two-phase) configuration. This improvement could be partially due to the pressure ratio, which was lowered by an average of 8 % when the intracycle heat exchanger was used with two-phase exiting the evaporator. At capacities above 7.0 kW (24 000 Btu/h) it actually performed better than R290 and R22-REF.

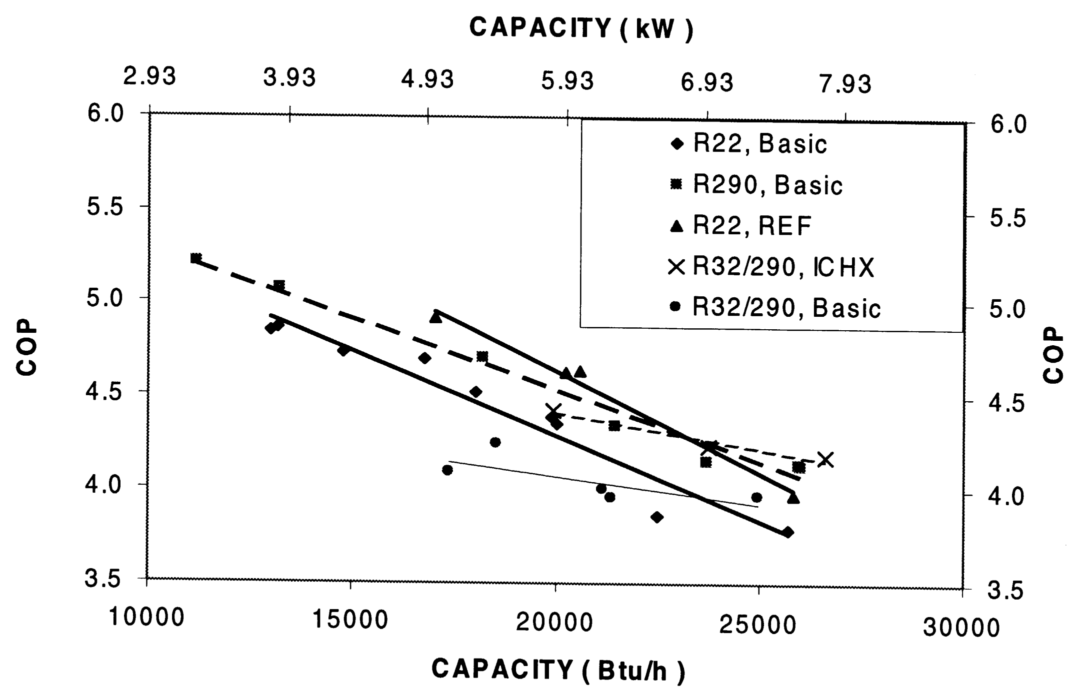

Figure 4.6: Comparison of heating COP's for R22, R290, and R32/290

5.0: Conclusions

R290 in the heating mode and R32/290 in the cooling mode produced the highest COPs in the simple cycle that excluded the internal heat exchanger. The addition of the internal heat exchanger with two-phase flow at the exit of the evaporator (ICHX configuration) improved COP for R32/290 in the cooling mode by as much as 5 %. However, the R32/290 with the ICHX could not equal the performance of R22-REF in the experimentally simulated direct expansion arrangement. COP for the R32/290 system with the internal heat exchanger was still 10 % below the R22-REF case. The additional ΔT required by the indoor heat transfer fluid loop could not be overcome using glide matching or an internal heat exchanger. In the cooling mode, all of the alternative refrigerants produced higher COPs than R22 when all the refrigerants were used in the same water-to-water configuration. R32/290 with the ICHX improved on the performance of R22 by 10 % ± 3 % throughout the capacity range tested. One added advantage of this 50/50 mixture by mass of R32/290 is its use of mineral oil in the compressor. Where regulations allow, R32/290 can provide an improvement over R22 in water-to-water heat pump applications.

The R290 basic heating mode test showed that the penalty in the heating mode of the extra HTF loop was less than that in the cooling mode. This was partially due to the evaporators being at the same condition for all of the refrigerants. Attempts to enhance COP using the internal heat exchanger with R290 failed. As opposed to improving COP, internal heat exchange produced performance degradation. The COP degradation was due to superheated conditions at the outlet of the heat exchanger on the vapor side and the added pressure drop of the internal heat exchanger. The same held for R290 in the cooling case. Additional testing should be performed with R290 and the R32/290 mixture over a wider range of temperature lifts (pressure ratios). This would allow a more informed comparison of the COP characteristics of these mixtures.

ACKNOWLEDGEMENTS

This project was jointly funded by NIST and the U.S. Department of Energy (project no. DE-AI01-97EE23775) under Project Manager Esher Kweller. Thanks go to the following NIST personnel for their constructive criticism of the first draft of this manuscript: Dr. M. Kedzierski and Mrs. M. Buckley. Thanks also to Dr. J. S. Brown and Dr. D. Olson for their reviews of this document.

REFERENCES

Choi, D. K., P. A. Domanski, and D. A. Didion. 1996. Evaluation of flammable refrigerants for use in a water-to-water residential heat pump. IIF – IIR Commissions B1, B2, E1, and E2 Conference. *Applications for natural refrigerants*. Aarhus, Denmark. September 3-6.

Kedzierski, M. A., Kim, J. H., and Didion, D. A., 1992, "Causes of the Apparent Heat Transfer Degradation for Refrigerant Mixtures," Two-Phase Flow and Heat Transfer, HTD-Vol.197, J. H. Kim, R. A. Nelson, and A. Hashemi, Eds., ASME, New York, pp. 149-158.

Domanski, P. A., D. A. Didion, and W. Mulroy. 1994. A simulation model and study of hydrocarbon refrigerants for residential heat pump systems. IIR Conference, Hanover, Germany, pp. 339-354.

Domanski, P.A. 1995. Theoretical Evaluation of the Vapor Compression Cycle With a Liquid-Line/Suction-Line Heat Exchanger, Economizer, and Ejector. NISTIR 5606. National Institute of Standards and Technology. Gaithersburg, MD. USA.

Domanski, P.A., Kim, B.S., 1996. Intracycle evaporative cooling in a vapor compression cycle. NISTIR 5873. National Institute of Standards and Technology. Gaithersburg, MD. USA.

Dow Chemical Company. 1995. Fluidfile 2.0 software program for Windows. Midland, Michigan, USA.

Mulroy, W., Kauffeld, M., McLinden, M., and Didion, D.A., 1988, Experimental Evaluation of Two Refrigerant Mixtures in a Breadboard Air Conditioner, Proceedings of the 2nd DOE/ORNL Heat Pump Conference, Washington, D.C.

NIST. 1996. *NIST thermodynamic properties of refrigerants and refrigerant mixtures database.* (REFPROP 5.16). Gaithersburg, MD. USA

Payne, W.V., Domanski, P.A., Muller, J., 1999. A study of a Water-to-Water heat pump using hydrocarbon and hydrofluorocarbon zeotropic mixtures. NISTIR 6330. National Institute of Standards and Technology. Gaithersburg, MD. USA.

Vakil, H., 1981. *Means and method for the recovery of expansion work in a vapor compression cycle device.* United States Patent No 4034099.